Hindawi
Journal of Spectroscopy
Volume 2023, Article ID 9911266, 7 pages
https://doi.org/10.1155/2023/9911266

Research Article

Study of the Hydration Mechanism of Portland Cement with Raman Spectroscopy Applying CO_2 Laser Radiation

D. Quiroz-Portillo,[1] **I. Rosales-Candelas**,[1] **J. J. Soto-Bernal**,[1] **R. González-Mota**,[2] **and G. V. Vázquez**[3]

[1]*Department of Electronic Engineering, TecNM/Instituto Tecnológico de Aguascalientes, Av Adolfo López Mateos Ote 1801, Bona Gens 20256, Aguascalientes, Mexico*
[2]*Department of Chemical and Biochemical Engineering, TecNM/Instituto Tecnológico Aguascalientes, Av Adolfo López Mateos Ote 1801, Bona Gens 20256, Aguascalientes, Mexico*
[3]*Department of Optical Fibers and Lasers, Centro de Investigaciones en Óptica, Lomas del Bosque 115, Lomas del Campestre 37150, León, Guanajuato, Mexico*

Correspondence should be addressed to D. Quiroz-Portillo; dquiroz@cycna.com.mx

Received 1 September 2022; Revised 21 March 2023; Accepted 31 March 2023; Published 15 April 2023

Academic Editor: Pedro D. Vaz

This work presents the results by irradiating fresh Portland cement pastes with CO_2 laser, at powers of 1.6, 2.0, and 2.4 W, at different water-to-cement (w/c) ratios 0.4, 0.45, and 0.5. Raman spectra show the evolution and accelerated growth of the main hydration products through the intensity changes of the Raman signal. The Raman shifts reveal that the C-S-H, CH, AFt, and $CaCO_3$ bands are detected in a shorter time, which means that the setting times are also reduced. The detected band of calcium carbonate, which is due to the incorporation of limestone during the grinding process, shows that it is responsible largely for the acceleration in the reactions during the hydration of the cement. The Raman signals of the hydration products of nonirradiated cement pastes present a delay in their evolution with respect to the irradiated pastes. The curves obtained from the Raman spectra can be used to model the mechanism of hydration as well as to understand the setting process.

1. Introduction

The study of the hydration mechanisms of cement and concrete is of great interest today, since they describe the behavior of the main components of the cement and the formation of the hydration products, which determine the quality of the Clinker and Portland cement. The main hydration products are calcium silicate hydrate (C-S-H), Portlandite (CH or $Ca(OH)_2$), ettringite (AFt), and monosulfate (AFm). Hydration is a highly exothermic process, which depends on several factors such as the fineness of the cement, its chemical composition, the w/c ratios, and the clinker cooling process inside the kiln, among others [1]. However, within the hydration process endothermic processes are carried out, such as the precipitation of CH [2]. The hydration reactions begin with the mixture of water with the different phases of the Clinker, such as the tricalcium silicates C_3S and dicalcium C_2S, as well as the tricalcium aluminate C_3A and the tetracalcium ferroaluminate C_4AF, together with calcium sulfate $CaSO_4.2H_2O$ known as gypsum, which is added in the grinding process to control the reaction of C_3A in the hydration of the paste [3]. These phases react simultaneously but at different speeds, although the reactions of each component of the mixture have an influence on each other [3]. The hydration mechanisms of Portland cement are divided into periods or stages known as preinduction, induction (dormant), acceleration, and deceleration, which have been modeled from the hydration of C_3S as it is the major component and the main contributor of the change in strengths in Portland cement, using calorimetry techniques and modeling of the changes in the development of the microstructure of the cement particles

through the Powers model, among others [4]. Other studies of hydration mechanisms have focused on the evolution of the microstructure of hydration products using techniques such as scanning electron microscopy (SEM) [5, 6]. Raman spectroscopy is an alternative analysis technique for the study of anhydrous and hydrated cements [7]. In the case of the study of hydrated cements, it has been shown to have potential due to its high spectral resolution and the fact that water does not fluoresce in the Raman effect, allowing the collection of hydrated phase bands without any type of masking of the signal [8]. Sulfates have been studied with Raman spectroscopy in ordinary Portland cement pastes and with fly ash in the infrared region 950–1050 cm^{-1}, since fluorescence is reduced in this region of the electromagnetic spectrum [9]. Raman spectroscopy has also been used to monitor the setting process in cement pastes, where bands of hydration products such as C-S-H, $Ca(OH)_2$, and AFt phase have been detected, as well as the main components of anhydrous cement [10]. One of the variables of interest in the hydration mechanisms is the strength at early ages in cement pastes and in concrete, which is attributed to several factors such as the C-S-H, the water-to-cement ratio and the intermolecular van der Waals forces. [11]. There are traditional methods to improve the strength of cements, either with some type of additive in the mixture or by varying of the w/c ratio [11, 12]. Moreover, there are studies where it has been possible to improve the mechanical properties and reduce the setting times with the application of CO_2 laser radiation in cement pastes [13, 14]. Also, there are studies about the quantification of C_3S and C_2S with thermal techniques [15]. This work shows the evolution and acceleration in the formation of hydration products in cement pastes by monitoring changes in their Raman spectra after CO_2 laser radiation which describe the mechanisms of Portland cement hydration. In addition, they also reveal the increase in the degree of hydration of the paste through changes in the $CaCO_3$ band, since the incorporation of calcium carbonate accelerates the hydration reactions, increasing its initial strength. The information obtained can be used to describe the behavior of the molecular microstructure and the mechanisms of the hydration process of the cement pastes irradiated by CO_2 laser, in order to improve the design of the mixtures of the raw material and the abundance of the aggregates. In this way, it would be possible to ensure the quality of the Clinker, the Portland cement, as well as the concrete.

2. Materials and Methods

2.1. Cement Paste Preparation. Composite Portland cement classified by the Mexican standard NMX-C-414 for CPC 30R RS cements was used for the preparation of pastes, as well as distilled water, employing the ASTM C 305 standard at different w/c ratios 0.4, 0.45, and 0.5.

2.2. Cement Paste Characterization. For the measurement of the fresh pastes a Raman DXR microscope with a full range diffraction grating and Mplan 10x/0.25 objective was used together with a laser with a wavelength of 780 nm at a power of 5 mW as excitation source. For the treatment of the Raman spectra, the Origin 2016 analysis software was used.

2.3. Cement Paste Irradiation. To irradiate the fresh cement pastes, an Engraver C120H model CO_2 laser was used at a wavelength of 10.6 micrometers (μm), with a spot diameter of 1.8 cm, at different powers: 1.6, 2.0, and 2.4 W measured with a Synrad power meter. A negative meniscus zinc selenide (ZnSe) lens was used to expand the spot. The size of the fresh paste sample was 5 cm in diameter with a thickness of 1 cm. The samples were mounted on a support 20 cm from the ZnSe lens. The pastes were irradiated on their upper surface, increasing the exposure time up to 8 hours, which is the estimated time to reach the final setting for this type of cement. The optical array used was sufficient to irradiate the entire sample. The sequence for the irradiation of the cement pastes was as follows: The cement paste was prepared and irradiated for 30 s, then removed from the CO_2 laser beam and measured with the Raman DXR microscope to obtain its Raman spectrum. The previous step was performed for the different irradiation times (1 min, 2 min, 4 min, 8 min, 15 min, 30 min, 1 h, 2 h, 3 h, 4, 5 h, 6 h, 7 h, 8 h). Figure 1 shows the optical arrangement used to irradiate the cement pastes with the CO_2 laser. It is important to note that the CO_2 laser is a molecular laser that emits at 10.6 μm in the mid-infrared region, for which it is necessary to use a zinc selenide lens, which has high transmittance at that wavelength.

3. Results and Discussion

Figures 2(a) and 2(b) show the Raman spectra of a cement paste irradiated with a CO_2 laser at a power of 1.6 W with w/c ratio of 0.45 during the first 8 hours of hydration of the paste. Figures 2(c) and 2(d) show a selection of 2(a) and (b) just in the range of 200 to 800 cm^{-1} in order to focus on the evolution of C-S-H during the acceleration stage because it is the main contributor of the change strengths in Portland cement. Raman spectra show the main hydration products such as hydrated calcium silicate C-S-H and Portlandite CH, as well as the presence of sulfates AFt, AFm, and $CaSO_4.2H_2O$. In addition, calcium carbonate $CaCO_3$ in the form of calcite was also recorded. In Raman shifts 451, 616, and 656 cm^{-1} C-S-H was detected, with Portlandite at 356 cm^{-1}, calcium hydroxide $Ca(OH)_2$ at 1532 cm^{-1}, AFt in the 989 cm^{-1} band, gypsum at 1002 cm^{-1}, $CaCO_3$ at the Raman band 1086 cm^{-1}, and in the region of 3300 cm^{-1} corresponding to the O-H tension bond due to the presence of water in the sample. Other researchers have already reported the assignments of these bands [16]. In the first two hours of hydration, C-S-H shows broad and weak bands due to its normal Si-O-Si strain-symmetric vibration modes and its poor crystallinity, showing that its molecular structure is disordered and that it is a compound with variable composition. As hydration progresses, the C-S-H forms an ordered molecular structure, and its bands become narrower and sharp, however, the Raman signal intensities vary from

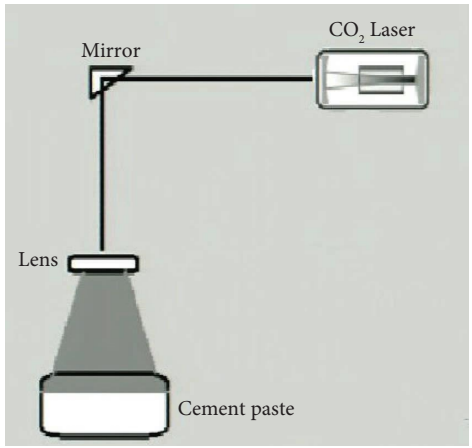

Figure 1: Optical arrangement to irradiate cement pastes with CO_2 laser.

strong to weak. This is because the propagation of the electric field of the CO_2 laser induces an effect on the water molecules that causes them to produce rotations and microvibrations due to the fact that water molecules are extremely polar and are aligned according to the orientation of the electric field in addition to having a nonlinear geometry, resulting in an acceleration in the modification of the crystallization and in the microstructure of the hydration products such as C-S-H, $Ca(OH)_2$, and AFt, which can be observed in the change in the shape and width of the bands, as well as in the intensities of the peaks, which are associated with certain vibrational modes. It can be seen that the Portlandite band undergoes slight increases, which could be due to the continuous dissolution of the cement phases as well as the precipitation of the hydration products during the setting stage. The presence of ettringite is attributed to the rapid reaction of C_3A with gypsum, since the hydration of C_3A consumes gypsum and consequently ettringite is produced. The presence of the AFm band may be due to the reaction of C_3A with the presence of ettringite because of the decrease or elimination of gypsum. However, it can be seen that the Raman bands of these sulfates undergo frequency shift changes, which can be attributed to the chemical reactions of the sulfates during the early stages of hydration. Raman spectra show the formation of calcium carbonate $CaCO_3$ in the form of calcite on the surface of the cement paste, due not only to the reaction of atmospheric CO_2 with Portlandite $Ca(OH)_2$, but also due to the addition of 20% limestone for this type of cement during the grinding process, mainly as $CaCO_3$. The addition of calcium carbonate accelerates the hydration reactions of Portland cement, increasing the initial strength (due to the formation of the C-S-H phase of an amorphous nature), the degree of hydration, and the amount of released CH, among others [17, 18].

The study includes a comparison of the evolution of the Raman signals for different irradiation powers while maintaining the w/c ratio. As mentioned before, the study is focused on C-S-H because it is the main contributor of the change in strengths in Portland cement, however, the evolution of AFt as well as $Ca(OH)_2$ is also shown to reveal the effect of CO_2 laser irradiation of these hydration products. Figures 3(a)–3(c) are obtained from the corresponding Raman spectra, showing the evolution of the main hydration products present in the cement paste during the first 480 minutes of hydration for nonirradiated pastes as well as irradiated pastes at different powers of the CO_2 laser at a w/c ratio of 0.45. In Figure 3(a), the evolution of C-S-H can be observed as hydration progresses, revealing its presence from the first minutes and an accelerated growth of the Raman signal from the first 90 minutes for the 2.4 W power, at 120 minutes for the power of 2.0 W, and for the power of 1.6 W after 150 minutes; for the sample without irradiation, the intensity of the Raman signal begins to increase after 180 minutes but with less intensity. However, at the age of 480 minutes of hydration, a decrease in the intensities of the Raman bands is recorded, which can be attributed to the decrease in water and the possible crystallization of the paste, possibly due to the fact that C-S-H is a phase of variable composition, which presents a structure in the form of finite chains of silicon tetrahedrons with an undefined stoichiometry. The accelerated growth of the Raman signal of the C-S-H is due not only to the influence that the electric field of the CO_2 laser radiation has on the water molecules but also because this type of radiation is strongly absorbed by water molecules, accelerating photophysical and physicochemical reactions in the molecular structure of the cement paste. Figure 3(b) shows the formation of AFt from the first minutes of hydration, due to the rapid reaction of gypsum with C_3A and water for both the irradiated and nonirradiated samples. The intensities of the Raman signals of the irradiated samples increase after 120 min, confirming the presence of AFt, which can be attributed to the fact that there is enough calcium sulfate to make the ettringite stable. It is observed that the Raman signal decreases in intensity at 360 min for the 2.4 W power and at 420 min for 2.0 W, because the ettringite becomes unstable, causing the formation of AFm due to the fact that there could be an excess of C_3A and a decrease in gypsum. Changes in the bands of the Raman peaks of ettringite can help to understand the hydration behavior during the setting stage. Reported studies [19] say that the setting of Portland cement is due to the re-crystallization of the primary microcrystalline ettringite crystals. This recrystallization is observed in the bands of the Raman spectra obtained since they become narrower due to the radiation induced by the CO_2 laser. The Raman bandwidth provides information on the crystallinity: the narrower the bands are, the more crystalline the material is. Figure 3(c) shows the evolution of Portlandite, which is formed due to the absorption of OH^- on the surface of Ca^{2+} in the cement paste. The maximum peak of the Raman signal for the three powers occurs at 420 min of the hydration of the paste, which implies the acceleration period and the formation of large amounts of Portlandite. However, the Raman signal of the nonirradiated paste just began to increase, indicating a delay in its formation; it is worth mentioning that its contribution to the strength of the cement is minimal because the forces of its bonds are relatively weak for both irradiated and

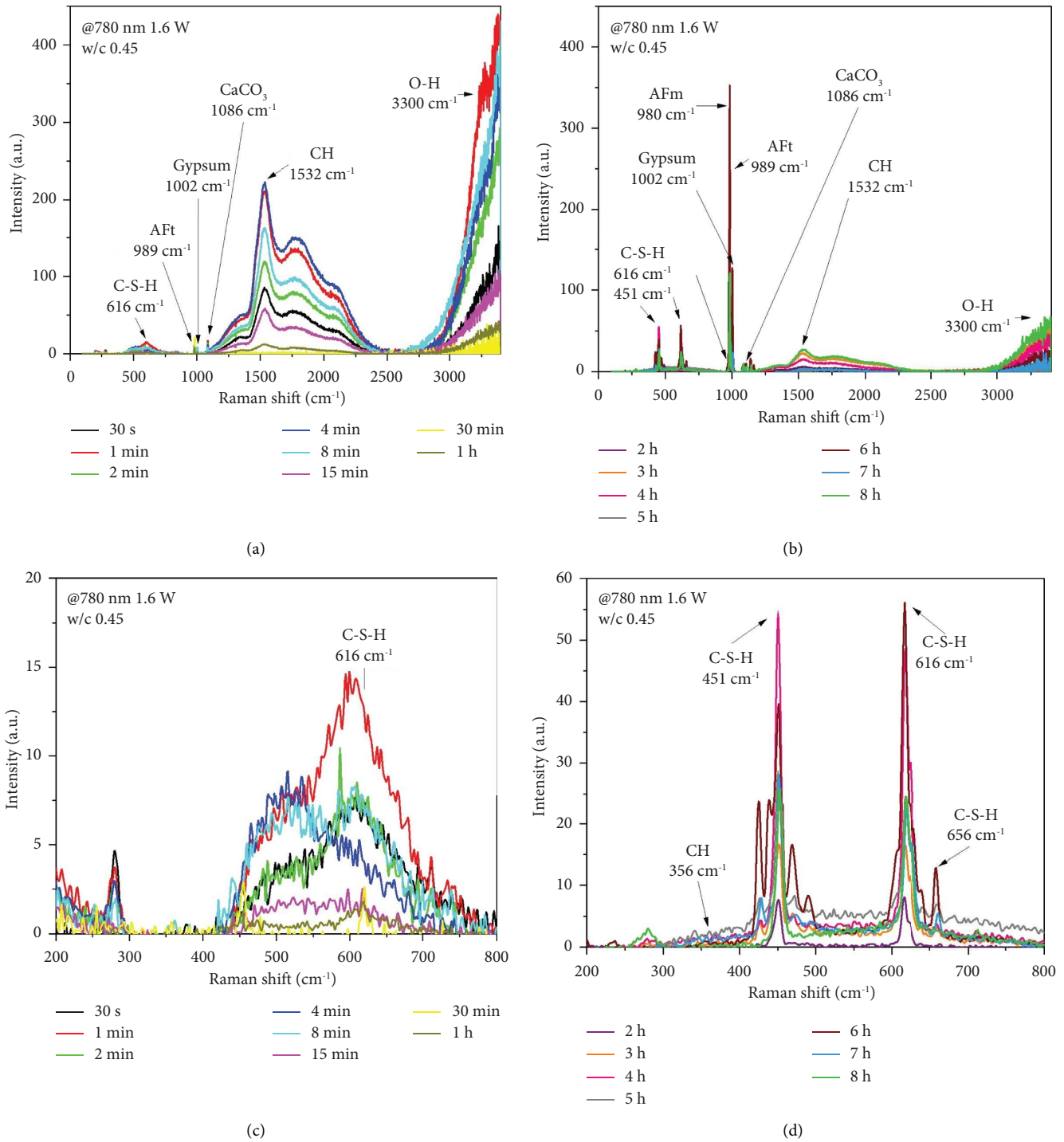

Figure 2: Raman spectra of paste irradiated with CO_2 laser at 1.6 W with w/c ratio 0.45. (a) Raman spectra from 30 s to 1 h of irradiation. (b) Raman spectra from 2 h to 8 h of irradiation. (c) Evolution of C-S-H from 30 s to 1 h. (d) Evolution of C-S-H and CH from 2 to 8 h.

nonirradiated samples. From these results, Raman spectra of irradiated samples reveal that Portland cement paste experiences acceleration in the crystallization of C-S-H and AFt, indicating that the setting time happens in a shorter time due to the influence of the electric field of the CO_2 laser on the water molecules. Also, irradiated samples indicate a paste with fewer pores, which can be attributed to an increase in the strength of the sample. However, the Raman spectra without irradiation show that the crystallization of the paste occurs over longer periods of time. Also, the paste shows more porosity.

The graphs reveal an inverse relationship of the powers used and the rise times of the Raman signal intensities; the increase in power reduces the evolution time of the C-S-H; this may be because the dormant period is reduced, stimulating the acceleration period, which is where the C-S-H gel

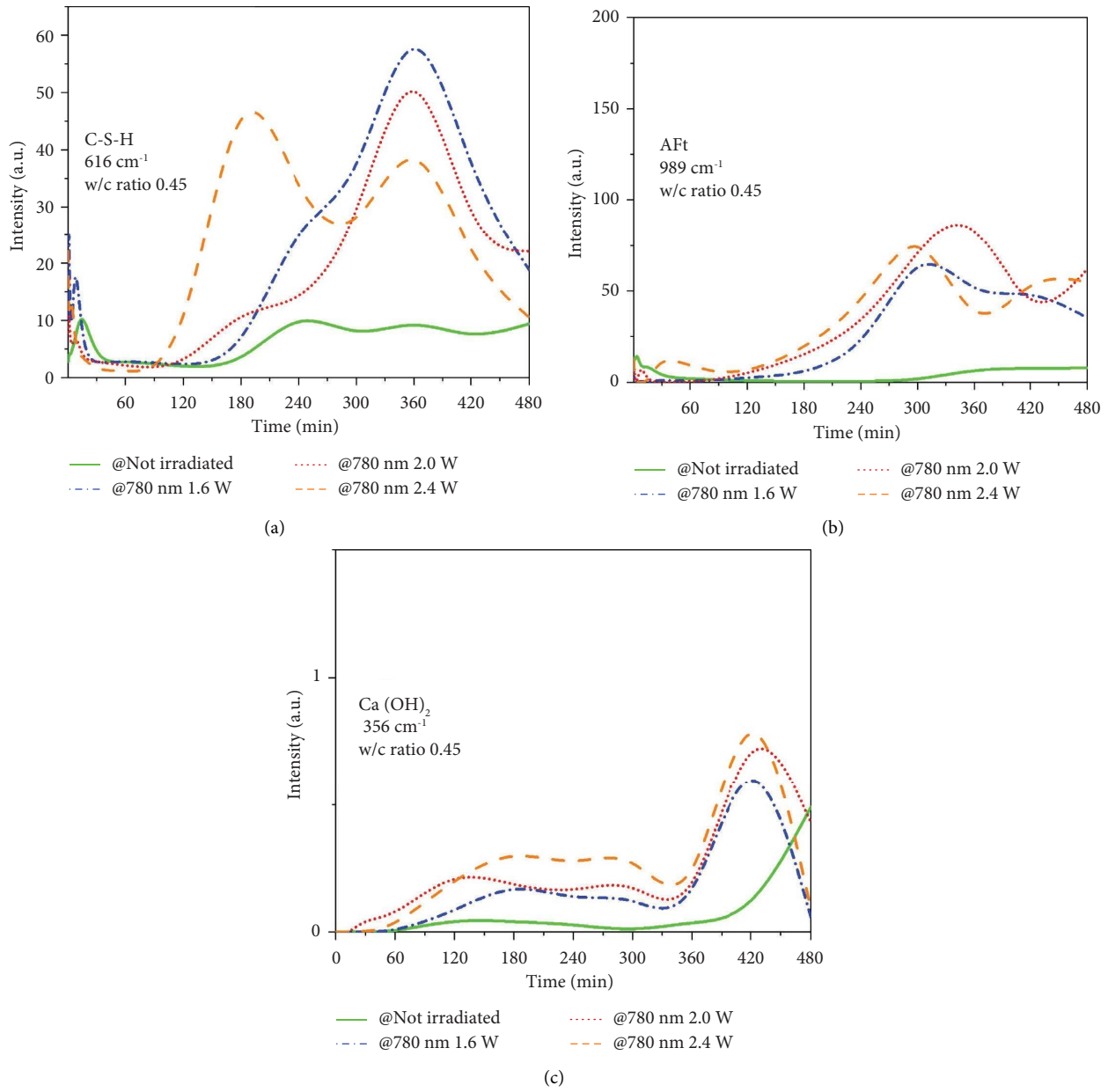

Figure 3: Evolution of the Raman signal of the main hydration products, for irradiation at 1.6, 2.0, and 2.4 W and without irradiation with a w/c ratio 0.45, (a) C-S-H. (b) AFt. (c) $Ca(OH)_2$.

grows very quickly. We also compared the evolution of the Raman signal for the different w/c ratios, keeping the irradiation power constant. Figures 4(a)–4(c) show the evolution of C-S-H through the changes in the intensities of the Raman signal in the 616 cm^{-1} band of cement paste samples irradiated with CO_2 laser for 1.6, 2.0, and 2.4 W, at different w/c ratios 0.4, 0.45, and 0.5 during the first 480 minutes after sample preparation. It can be seen that for the w/c ratio of 0.4, the intensity of the Raman signal begins to increase slightly before the other w/c 0.45 and 0.5: at 120 min for the power of 1.6 W, at 90 min for 2.0 W and at 80 minutes for 2.4 W, where the Raman signal reveals the formation of large amounts of C-S-H gel, which could be the beginning of the paste setting process. It is also observed that after 360 min of paste hydration, the intensity of the Raman signal decreases for the three powers due to a possible crystallization of the paste. The changes in the band of the Raman signal of the C-S-H from the first minutes of contact of the cement particles with the water molecules suggest a rapid dissolution of the C_3S and C_3A, as well as the sulfates present in the cement paste, possibly causing the early appearance of C-S-H gel. The Raman signal in the 616 cm^{-1} band was found in all the cement pastes at all w/c ratios, 0.4, 0.45, and 0.5 but its detection or appearance was at different ages of hydration. Raman spectra indicate that for all irradiation powers at a w/c ratio 0.5, the 616 cm^{-1} band is detected relatively later compared to 0.4 and 0.45 w/c ratios. This is because the cement paste with a higher w/c ratio may undergo a longer

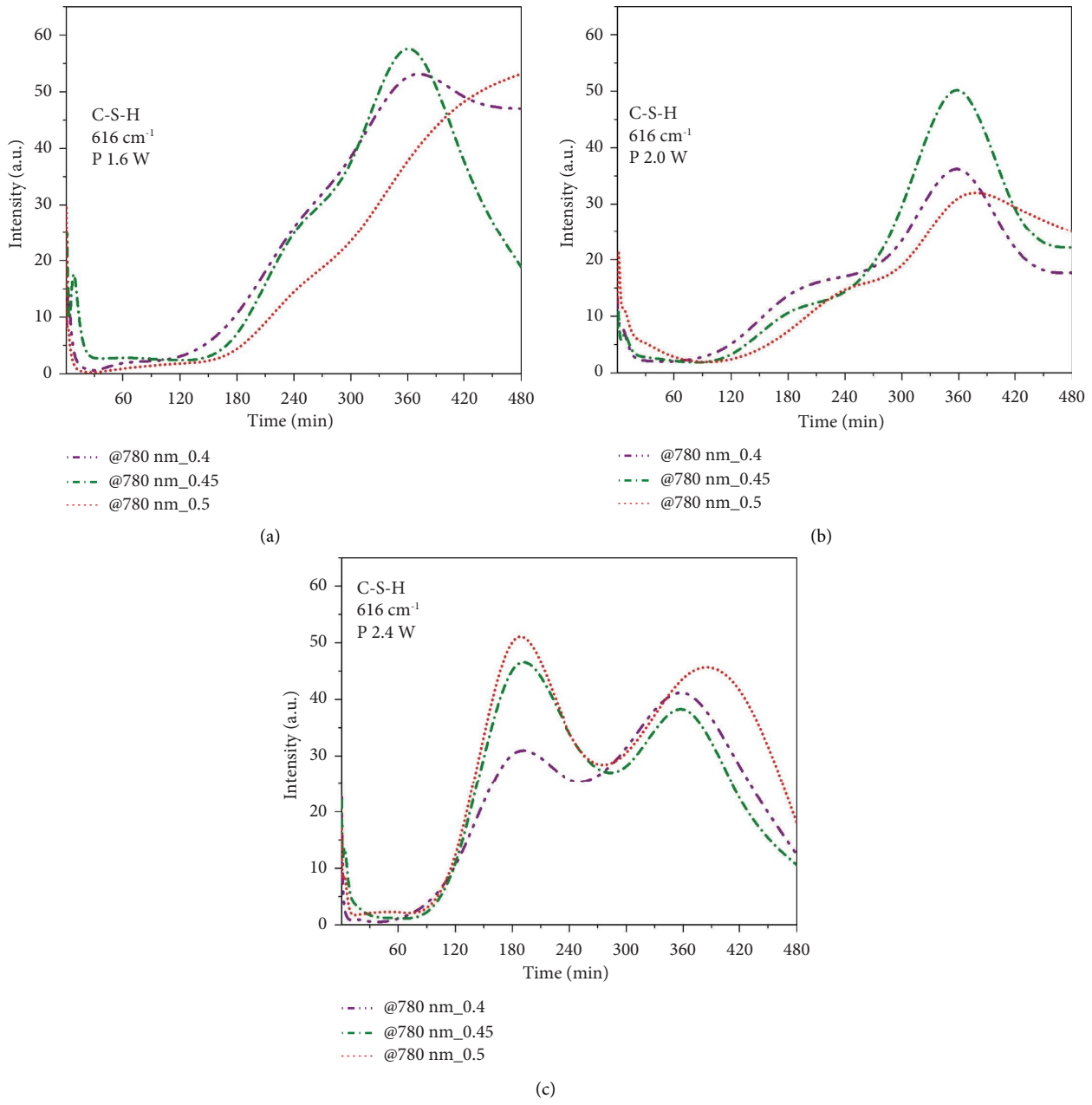

Figure 4: Evolution of the Raman signal of C-S-H, in the cement paste irradiated at different powers and w/c ratios. (a) 1.6 W. (b) 2.0 W. (c) 2.4 W.

dormant period which may cause a delay in the hydration of C_3S and consequently a delayed formation of C-S-H gel; in the dormant period, the reaction rate decreases and the heat release is significantly reduce. Also by increasing the irradiation power the dormant period can be reduced, as shown before in Figure 3(a). Indeed at a power of 2.4 W the dormant period is considerably reduced and the acceleration stage occurs achieving crystallization of the paste in less time, and the signal Raman is stronger and narrower at 180 minutes, forming large amounts of C-S-H gel. At 370 minutes the Raman signal becomes stronger again, which means a new acceleration in the speed in the dissolution of the C_3S, followed by an increase in the heat released due to the massive formation of ettringite.

4. Conclusions

In this work, we demonstrate that by irradiating with a CO_2 laser at a wavelength of 10.6 μm on fresh Portland cement pastes and increasing the irradiation power, hydration mechanisms undergo an acceleration in their chemical reactions. This effect can be seen in the fact that the times for the detection of the Raman bands of the hydration products as well as their evolution are short compared to

nonirradiated fresh paste samples. According to Raman spectra, the setting times are also reduced by increasing the irradiation power on the fresh pastes. The C-S-H gel, which is characterized by being a poorly crystalline phase and of variable composition, experiences improvements in its crystallinity according to the bands recorded. The curves obtained in this work, which show the evolution of the Raman signal after CO_2 laser irradiation, can be used to model the hydration mechanisms through the C-S-H instead of using the C_3S used by other methods.

Data Availability

The data used to support the findings of this study are available from the first author upon request.

Conflicts of Interest

The authors declare that they have no conflicts of interest.

Acknowledgments

The authors are grateful to the Technological Institute of Aguascalientes for providing materials and equipment.

References

[1] K. L. Scrivener and A. Capmas, *Lea" S Chemistry of Cement and Concrete*, Vol. 58, Elsevier science, Amsterdam, Netherlands, Fourth edition, 2004.

[2] K. L. Scrivener, P. Juilland, J. Paulo, and M. Monteiro, "Advances in undesrtanding hydration of portland cement," *Cement and Concrete Research*, vol. 78, 2015.

[3] J. W. Bullard and M. J. Hamlin, "Mechanisms of cement hydration," *Cement and Concrete Research*, vol. 41, 2011.

[4] L. S. Karen and A. Nonat, "Hydration of cementitius materials, present and future," *Cement and Concrete Research*, vol. 41, 2011.

[5] M. Manuel Alejandro Giraldo and J. Ivan Tobon, *Mineralogical Evolution of Portland Cement during Hydration Process*, Universidad nacional de colombia, Medellin, 2005.

[6] M. Fengjuan Liu, "Early-age hydration studies of Portland cement," University of Louisville, Louisville, KY, USA, Tesis Doctoral, 2014.

[7] S. Martinez Ramirez and L. Fernandez Carrasco, "Estudio de los cementos anhidros e hidratados a traves de espectroscopia Raman," *Revista tecnica cemento hormigon*, vol. 942, 2011.

[8] G. Renaudin, R. Segni, D. Mentel, J. M. Nedelec, F. Leroux, and C. Taviot-Gueho, "A Raman study of the sulfated cement hydrates: ettringite and Monosulfoaluminate," *Journal of Advanced Concrete Technology*, vol. 5, no. 3, pp. 299–312, 2007.

[9] N. Garg, K. Wang, and S. W. Martin, "A Raman spectroscopic study of the evolution of sulfates and hydroxides in cement–fly ash pastes," *Cement and Concrete Research*, vol. 53, pp. 91–103, 2013.

[10] F. Llu and Z. Sun, "Raman spectroscopy study on the hydration behaviors of Portland cement pastes during setting," *Journal of Materials in Civil Engineering*, vol. 27, 2014.

[11] G. Guevara Fallas, C. Hidalgo Madrigal, M. Pizarro García, I. Rodríguez Valenciano, L. D. Rojas Vega, and G. Segura Guzmán, "Efecto de la variación agua/cemento en el concreto," *Revista Tecnología en Marcha*, vol. 25, no. 2, p. 80, 2012.

[12] D. M. Kirby, J. J. Biernacki, and G. S. Guzman, "The effect of water to cement ratio on the hydration kinetics of tricalcium silicate cement," *Cement and Concrete Research*, vol. 42, 2012.

[13] M. R. Moreno Virgen, J. J. Soto Bernal, and J. A. Ortiz Lozano, "Effect of CO_2 laser radiation on the mechanical properties of Portland cement pastes," *Materiales de Construcción*, vol. 61, no. 301, pp. 77–91, 2010.

[14] M. R. Moreno Virgen, J. J. Soto Bernal, and J. A. Ortiz Lozano, "Laser radiation CO_2, effects in cement paste at different hydration stages after preparation," *Ingeniería: Investigación y Tecnología*, vol. 12, no. 3, 2011.

[15] S. Goñi, J. J. F. Puertas, and M. S. Hernandez, "Quantitative study of Hydration of C_3S and C_2S by thermal analysis," *Journal of Thermal Analysis and Calorimetry volume*, vol. 102, 2010.

[16] L. Black, *Raman Spectroscopy of Cementitious Materials*, The Royal Society of Chemistry, London, UK, 2009.

[17] P. L. Valdez Tamez, A. Duran Herrera, G. Fajardo San Miguel, and C. A. Juarez Alvarado, "Carbonatation influence on fly ash and Portland cement mortars," *Ingeniería: Investigación y Tecnología*, vol. 10, 2009.

[18] V. F. Rahhal, V. L. Bonavetti, and R. Talero, "Early hydration of cements with medium and hight content of crystaline mineral admixtures," 2015, https://repositorio.uc.cl/handle/11534/11346.

[19] J. A. Ortiz, J. Rocero, and M. E. Zermeño, "Influencia de la temperatura ambiental sobre las propiedades de trabajabilidad y microestructurales de morteros y pastas de cemento," *Revista Cemento y Concreto. Investigación y Desarrollo*.vol. 1, 2009.